ESR Characterization of the Organic Superconducting Salts of the BEDT-TTF Donor Molecule with the Novel Organometallic Anion $[Cu(CF_3)_4]^-$ [BEDT-TTF = Bis(ethylenedithio)tetrathiafulvalene]

H. Hau Wang,* John A. Schlueter, Urs Geiser, and Jack M. Williams

Chemistry and Materials Science Divisions, Argonne National Laboratory, Argonne, Illinois 60439

D. Naumann and T. Roy

Institut für Anorganische Chemie, Universität Köln, Greinstrasse 6, D-50939 Köln, Germany

Received May 25, 1995[⊗]

Two new organic superconductors and a semiconductor were the subject of angular- and temperature-dependent ESR (electron spin resonance) studies. The low-T_c (4.0 K) κ_L-$(ET)_2Cu(CF_3)_4(TCE)$ phase gave room-temperature line widths and g values between 68 ($\Delta H_{||}$) and 54 ($\Delta H_{\perp}$) G and between 2.0052 ($g_{||}$) and 2.0097 ($g_{\perp}$), respectively. Its low-temperature behavior can be qualitatively correlated to four-probe resistivity measurements and described with the use of Elliott's formula. The high-T_c (9.2 K) κ_H-$(ET)_2Cu(CF_3)_4(TCE)$ phase gave a narrow line width range of 6.2 ($\Delta H_{||}$) to 5.8 ($\Delta H_{\perp}$) G and corresponding g values of 2.0081 ($g_{||}$) to 2.0105 ($g_{\perp}$), respectively. The solvent-free semiconductor $(ET)_2Cu(CF_3)_4$ revealed a characteristic line width between 30 and 40 G, thus providing a facile characterization of the three $ET/Cu(CF_3)_4^-$ phases based on their ESR peak-to-peak line widths. X-ray studies on the semiconductor indicated a similar unit cell compared to the previously reported α-$(ET)_2Ag(CF_3)_4$ phase. Superconducting κ_L- and κ_H-$(ET)_2Cu(CF_3)_4(TCE)$ crystals lost their cocrystallized solvent, TCE, at 340 and 380 K, respectively, and were converted to semiconducting $(ET)_2Cu(CF_3)_4$, indicating the close relationship among these three compounds.

Introduction

Organic superconductors have been studied actively in recent years.[1-3] The highly purified and crystalline nature of the electrochemically synthesized materials makes these novel systems ideal for various physical measurements. They also offer the potential for electronic device applications. More than two dozen BEDT-TTF [bis(ethylenedithio)tetrathiafulvalene, abbreviated "ET"] based organic superconductors have been reported to date. Nearly half of these superconductors belong to the κ-phase structural class, which often possesses relatively high superconducting transition temperatures (T_c's) among the organic superconductors, including the record for cation-radical salts. The prototype κ-phase crystal packing motif consists of sheets of face-to-face stacked ET dimers with neighboring dimers tilted at an approximately 90° angle. This packing arrangement creates a two-dimensional donor molecule layer possessing nearly isotropic physical properties parallel to the layer. The anions are located between the organic donor molecule layers. Among the κ-phase materials reported earlier are κ-$(ET)_2I_3$[4,5] and κ-$(ET)_4Hg_{3-\delta}X_8$ (X = Cl, Br),[6,7] followed by κ-$(ET)_2Cu(NCS)_2$.[8] The highest-T_c cation-radical salts belong to the κ-$(ET)_2Cu[N(CN)_2]X$ (X = Cl, Br) family.[9,10]

Recently, we reported a new family of κ-phase superconductors, i.e., κ-$(ET)_2M(CF_3)_4(Sol)$ (M = Cu, Ag, Au; Sol is cocrystallized 1,1,2-trihaloethane solvent),[11-15] which fall into

[⊗] Abstract published in *Advance ACS Abstracts,* October 1, 1995.

(1) Williams, J. M.; Ferraro, J. R.; Thorn, R. J.; Carlson, K. D.; Geiser, U.; Wang, H. H.; Kini, A. M.; Whangbo, M.-H. *Organic Superconductors (Including Fullerenes): Synthesis, Structure, Properties and Theory*; Prentice Hall: Englewood Cliffs, NJ, 1992.
(2) Williams, J. M.; Schultz, A. J.; Geiser, U.; Carlson, K. D.; Kini, A. M.; Wang, H. H.; Kwok, W.-K.; Whangbo, M.-H.; Schirber, J. E. *Science* **1991**, *252*, 1501.
(3) Ishiguro, T.; Yamaji, K. *Organic Superconductors*; Springer-Verlag: Berlin, Heidelberg, 1990.
(4) Kobayashi, A.; Kato, R.; Kobayashi, H.; Moriyama, S.; Nishio, Y.; Kajita, K.; Sasaki, W. *Chem. Lett.* **1987**, 459.
(5) Kato, R.; Kobayashi, H.; Kobayashi, A.; Moriyama, S.; Nishio, Y.; Kajita, K.; Sasaki, W. *Chem. Lett.* **1987**, 507.
(6) Lyubovskaya, R. N.; Lyubovskii, R. B.; Shibaeva, R. P.; Aldoshina, M. Z.; Gol'denberg, L. M.; Rozenberg, L. P.; Khidekel', M. L.; Shul'pyakov, Y. F. *Pis'ma Zh. Eksp. Teor. Fiz.* **1985**, *42*, 380 (*JETP Lett. (Engl. Transl.)* **1985**, *42*, 468).
(7) Lyubovskaya, R. N.; Zhilyaeva, E. I.; Pesotskii, S. I.; Lyubovskii, R. B.; Atovmyan, L. O.; D'yachenko, O. A.; Takhirov, T. J. *Pis'ma Zh. Eksp. Teor. Fiz.* **1987**, *46*, 149 (*JETP Lett. (Engl. Transl.)* **1987**, *46*, 188).
(8) Urayama, H.; Yamochi, H.; Saito, G.; Nozawa, K.; Sugano, T.; Kinoshita, M.; Sato, S.; Oshima, K.; Kawamoto, A.; Tanaka, J. *Chem. Lett.* **1988**, 55.
(9) Kini, A. M.; Geiser, U.; Wang, H. H.; Carlson, K. D.; Williams, J. M.; Kwok, W. K.; Vandervoort, K. G.; Thompson, J. E.; Stupka, D. L.; Jung, D.; Whangbo, M.-H. *Inorg. Chem.* **1990**, *29*, 2555.
(10) Williams, J. M.; Kini, A. M.; Wang, H. H.; Carlson, K. D.; Geiser, U.; Montgomery, L. K.; Pyrka, G. J.; Watkins, D. M.; Kommers, J. M.; Boryschuk, S. J.; Strieby Crouch, A. V.; Kwok, W. K.; Schirber, J. E.; Overmyer, D. L.; Jung, D.; Whangbo, M.-H. *Inorg. Chem.* **1990**, *29*, 3262.
(11) Schlueter, J. A.; Geiser, U.; Williams, J. M.; Wang, H. H.; Kwok, W.-K.; Fendrich, J. A.; Carlson, K. D.; Achenbach, C. A.; Dudek, J. D.; Naumann, D.; Roy, T.; Schirber, J. E.; Bayless, W. R. *J. Chem. Soc., Chem. Commun.* **1994**, 1599.
(12) Schlueter, J. A.; Carlson, K. D.; Williams, J. M.; Geiser, U.; Wang, H. H.; Welp, U.; Kwok, W.-K.; Fendrich, J. A.; Dudek, J. D.; Achenbach, C. A.; Naumann, D.; Roy, T.; Schirber, J. E.; Bayless, W. R. *Physica C (Amsterdam)* **1994**, *230*, 378.
(13) Schlueter, J. A.; Carlson, K. D.; Geiser, U.; Wang, H. H.; Williams, J. M.; Kwok, W.-K.; Fendrich, J. A.; Welp, U.; Keane, P. M.; Dudek, J. D.; Komosa, A. S.; Naumann, D.; Roy, T.; Schirber, J. E.; Bayless, W. R.; Dodrill, B. *Physica C (Amsterdam)* **1994**, *233*, 379.
(14) Schlueter, J. A.; Williams, J. M.; Geiser, U.; Dudek, J. D.; Kelly, M. E.; Sirchio, S. A.; Carlson, K. D.; Naumann, D.; Roy, T.; Campana, C. F. *Adv. Mater.* **1995**, *7*, 634.
(15) Schlueter, J. A.; Williams, J. M.; Geiser, U.; Dudek, J. D.; Sirchio, S. A.; Kelly, M. E.; Gregar, J. S.; Kwok, W.-K.; Fendrich, J. A.; Schirber, J. E.; Bayless, W. R.; Naumann, D.; Roy, T. *J. Chem. Soc., Chem. Commun.* **1995**, 1311.

0020-1669/95/1334-5552$09.00/0

distinct categories: the low-T_c κ_L-phases with platelike morphology and T_c's in the range 2.1−4.0 K and the high-T_c κ_H-needles with T_c between 9.2 and 11 K. In contrast to the low-T_c (κ_L) phase,[11,16] the high-T_c (κ_H) phase has not been structurally characterized due to the lack of suitable single crystals. In this article, we report the normal-state ESR properties of both κ_L- and κ_H-$(ET)_2Cu(CF_3)_4(TCE)$ (TCE is 1,1,2-trichloroethane), a new semiconducting phase, $(ET)_2Cu(CF_3)_4$, and the relationship among these three phases.

Experimental Section

The synthesis of the κ_L- and κ_H-$(ET)_2Cu(CF_3)_4(TCE)$ compounds was carried out with the use of the electrocrystallization technique, as previously reported.[11,12] The κ_L-phase crystals had a thin hexagon platelike morphology while the κ_H-phase grew as needles. These samples were stored with dry ice to avoid the loss of cocrystallized TCE solvent that occurs slowly at ambient temperature. The new $(ET)_2Cu(CF_3)_4$ phase crystallized simultaneously in some of the electrocrystallization cells as chunky hexagons and was identified by a distinct 30−40 G ESR line width at room temperature and by use of single-crystal X-ray diffraction techniques.

The ESR measurements were performed with the use of an IBM ER-200 X-band spectrometer with a TE_{102} rectangular cavity. Low-temperature experiments (4−300 K) were carried out with the use of an Oxford 900 flow-through cryostat and high-temperature measurements (300−450 K), with a 4111VT variable-temperature controller. A strong-pitch standard ($g = 2.0028$) was used for g value calibration. In order to carry out least-squares fitting of the line shapes, the original chart-recorder ESR spectra were digitized at a 400−500 data points/spectrum resolution with the use of the program Un-Plot-It (Silk Scientific, Inc.) and analyzed with the use of a Macintosh IIci with the KaleidaGraph (Synergy Software) data analysis software.

Single-crystal X-ray diffraction experiments were carried out by use of a Nicolet P3 four-circle diffractometer modified by the Crystallogic interface package. Graphite-monochromatized Mo Kα radiation (λ = 0.7107 Å) was used throughout. The crystal structure of κ_L-$(ET)_2Cu(CF_3)_4(TCE)$ has been reported,[11,16] and we have previously commented on the difficulties of obtaining lattice parameters, much less a complete structure, of κ_H-$(ET)_2Cu(CF_3)_4(TCE)_x$.[14] Most crystals of the solvent-free $(ET)_2Cu(CF_3)_4$ phase were heavily twinned in a lamellar fashion, often with gaps between. A very small fragment sufficiently single for a determination of the lattice parameters [monoclinic, a = 4.9975 (14) Å, b = 10.578(4) Å, c = 35.496(11) Å, β = 94.29(2)°, V = 1871.2 (1.0) Å^3], but too small for an intensity data collection, was finally found. The lattice parameters suggest that the crystals are isomorphous with $(ET)_2Ag(CF_3)_4$,[17] which, surprisingly, lacks the twinning problem and grows sizable, well-formed crystals.

Results and Discussion

(A) Orientation Study at Room Temperature. 1. κ_L-$(ET)_2Cu(CF_3)_4(TCE)$. The κ_L-$(ET)_2Cu(CF_3)_4(TCE)$ sample (a single hexagon plate) was oriented with the highly conducting *ac* plane vertical and *b* axis horizontal in the ESR cavity. The crystal was rotated around an arbitrary axis within the *ac*-plane since the physical properties parallel to the conducting *ac* plane are nearly isotropic. Angles 0 and 90° refer to the static magnetic field orientation parallel and perpendicular to the *ac* plane, respectively. As shown in Figure 1, the ESR signal can be described accurately with a single Lorentzian absorption.[18] The angular dependence of the peak-to-peak line widths and g values of the same crystal are plotted in Figure 2.

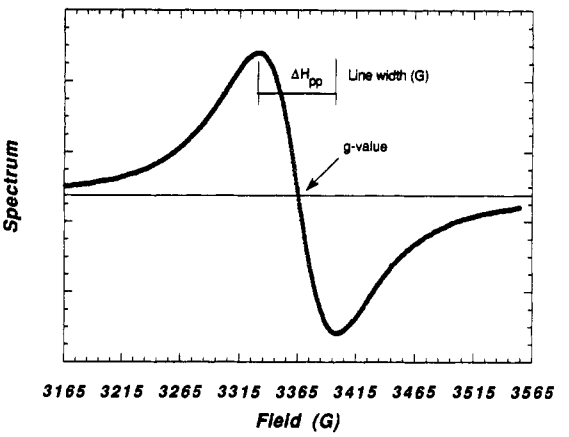

Figure 1. ESR signal of the κ_L-$(ET)_2Cu(CF_3)_4(TCE)$ crystal at 0° angle (circles). The calculated spectrum based on a single Lorentzian absorption is indicated with a solid line.

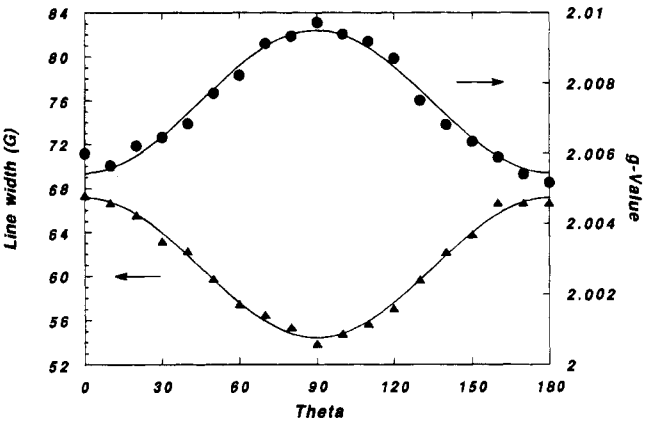

Figure 2. Angular-dependent peak-to-peak line widths (triangles) and g values (circles) of the κ_L-$(ET)_2Cu(CF_3)_4(TCE)$ phase. See text for fitted curves (thin lines).

The observed g values were fitted with use of the following equation:[19]

$$g_{obs}^2 = g_{||}^2 \sin^2\theta + g_x^2 \sin 2\theta + g_\perp^2 \cos^2\theta \qquad (1)$$

where g_{obs} is the observed g value, $g_{||}$ is the g value at 0° angle, $g_\perp$ is that at 90° angle, and g_x is a small cross term between parallel and perpendicular orientations in order to allow for a small orientation mismatch of the goniometer zero with the principal axes of the **g** tensor (see part B of Appendix). The peak-to-peak line widths, ΔH_{obs}, were also fitted with an analogous equation:

$$\Delta H_{obs} = (\Delta H_{||}) \sin^2\theta + (\Delta H_x) \sin 2\theta + (\Delta H_\perp) \cos^2\theta \qquad (2)$$

The calculated g values and line widths are drawn as thin lines in Figure 2, and the resultant line widths and g values varied from 68 ($\Delta H_{||}$) to 54 ($\Delta H_\perp$) G and from 2.0052 ($g_{||}$) to 2.0097 ($g_\perp$), respectively. The cross term values ΔH_x (0.004 G) and g_x (0.0084) are essentially zero in this case. The maximum g value occurs at 90° and corresponds to the minimum in peak-to-peak line width. This behavior is similar to that of other κ-phase materials, such as κ-$(ET)_2Cu[N(CN)_2]Br$,[20,21] κ-$(ET)_2Cu$-

(16) Geiser, U.; Schlueter, J. A.; Williams, J. M.; Naumann, D.; Roy, T. *Acta Crystallogr., Sect. B*, in press.
(17) Geiser, U.; Schlueter, J. A.; Dudek, J. D.; Williams, J. M.; Naumann, D.; Roy, T. *Acta Crystallogr., Sect. C*, in press.
(18) Poole, C. P., Jr. *Electron Spin Resonance: A Comprehensive Treatise on Experimental Techniques*; Interscience Publishers: New York, 1967; Chapter 10. See part A of Appendix for details.
(19) Drago, R. S. *Physical Methods in Chemistry*; W. B. Saunders Co.: Philadelphia, PA, 1977.
(20) Wang, H. H.; Beno, M. A.; Carlson, K. D.; Geiser, U.; Kini, A. M.; Montgomery, L. K.; Thompson, J. E.; Williams, J. M. In *Organic Superconductivity*; Kresin, V., Little, W. L., Eds.; Plenum Press: New York, 1990; pp 51.

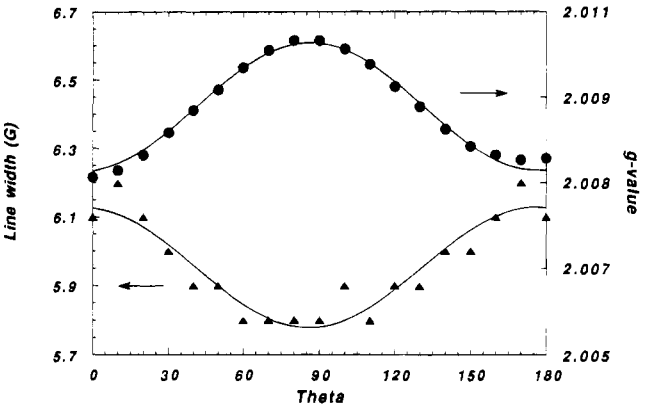

Figure 3. Angular-dependent peak-to-peak line widths (triangles) and g values (circles) of the κ_H-$(ET)_2Cu(CF_3)_4(TCE)$ phase.

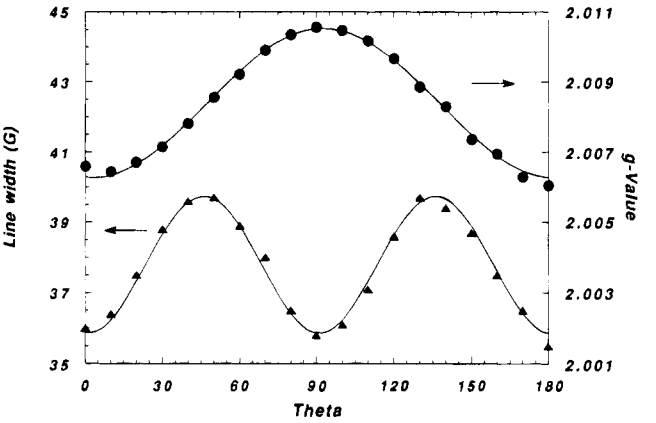

Figure 4. Angular-dependent peak-to-peak line widths (triangles) and g values (circles) of the $(ET)_2Cu(CF_3)_4$ phase.

$(NCS)_2$,[22] and κ-$(ET)_2Cu_2(CN)_3$.[23] The maximum g value near 90° is common to all two-dimensional layered ET salts, due to the largest g value contribution along the central C=C double bond in ET molecules.[24] The minimum line width near 90° is characteristic of the κ-phase salts and allows one to differentiate between α- and κ-phase ET salts even though the line widths are very similar for these two phases.[20]

2. κ_H-$(ET)_2Cu(CF_3)_4(TCE)$. A κ_H-$(ET)_2Cu(CF_3)_4(TCE)$ sample (multiply twinned needlelike platelet) was mounted vertically in the cavity. The crystal was rotated around its needle axis with 0° indicating that the static magnetic field was parallel to the crystal plane and 90° indicating that it was perpendicular to the crystal plane. In contrast to that of the κ_L-phase, the ESR signal from the κ_H-$(ET)_2Cu(CF_3)_4(TCE)$ phase at 0° refined well only with the use of a superposition of two Lorentzian absorptions,[18] the major one with a line width of 6 G and the minor with a 33 G width. The latter corresponds to the $(ET)_2Cu(CF_3)_4$ phase (*vide infra*). The integrated area for the major component was ~70%. At 90°, both components became sharper, such that the spectrum was dominated by the narrow-line component and could only be refined well with one absorption line. This behavior has been reported previously in the mixed α/β-$(ET)_2I_3$ system; i.e., the broader line can be overwhelmed by the sharper line, if the sharper component exceeds 60%.[25] Since the sharper 6 G line corresponded to the component of interest, we carried out the orientation study on the as-grown κ_H-$(ET)_2Cu(CF_3)_4(TCE)$ needle phase under this condition, and the result based on the apparent line widths and g values should be a valid representation of the κ_H phase. The peak-to-peak line widths (triangles) and g values (circles) are presented in Figure 3.

Again, the observed values were fitted with the use of eqs 1 and 2.[19] The calculated Lorentzian line widths and g values (indicated as thin lines) varied between 6.2 ($\Delta H_{\|}$) and 5.8 ($\Delta H_{\perp}$) G and between 2.0081 ($g_{\|}$) and 2.0105 ($g_{\perp}$), respectively. The maximum g value appeared near 90°, indicating a layered structure.[24] The minimum peak-to-peak line width also occurred near 90°, and the overall angular dependence of the line width and g value of the κ_H phase was quite similar to that of the κ_L phase, but with a much narrower line width range.

3. $(ET)_2Cu(CF_3)_4$. The third phase studied, identified with a distinct line width near 35 G, also had a hexagonal platelet morphology. The $(ET)_2Cu(CF_3)_4$ crystal was oriented vertically in the ESR cavity. The crystal was rotated around an arbitrary axis in the crystal plane, with the 0° angle indicating that the static magnetic field was parallel to the crystal plane and 90° angle indicating it was perpendicular to the plane. The ESR signal could be fitted well with use of a single Lorentzian absorption.[18] The observed g values and line widths are shown in Figure 4.

The peak-to-peak line widths and g values varied from 35 to 40 G and from 2.0061 to 2.0106, respectively. The observed g values were fitted well with the use of eq 1, while the observed double maximum in the line widths clearly cannot be described with eq 2. The maximum g value near 90° indicated that this sample belonged to a layered structure as suggested by the structural analysis of the isomophous Ag salt.[17] The line width data were phenomenologically fitted with a modified eq 2 by replacing all θ angles with 2θ. This behavior of a doubled periodicity in line width but not in g value was quite different from that of the κ_L and κ_H phases. At 0 and 180°, the observed line widths were clearly not the maximum line width. One likely explanation of this double periodicity is that there is a twinning problem (*vide supra*) within the crystal plane of this sample. To verify this possibility, a duplicate orientation study was carried out on the same crystal with the crystal rotated around a slightly different axis in the crystal plane. The result was similar to that shown in Figure 4, but the difference was a shallower local minimum in the line width near 90°. This observation suggested that the double periodicity was an artifact which could be caused by crystal twinning in a lamellar fashion so that the axes normal to the crystal planes of each twinned component are slightly misaligned. Better measurements must await a true single crystal.

(B) Low-Temperature Study. 1. κ_L-$(ET)_2Cu(CF_3)_4(TCE)$. The low-temperature (4−300 K) ESR spectra of a κ_L-$(ET)_2Cu(CF_3)_4$ (TCE) crystal were measured with the sample oriented at the 90° orientation (*vide supra*). The line widths increased upon cooling from 54 G at room temperature to 86 G near 100 K and then decreased rapidly to ~49 G at 10 K. The spin susceptibility decreased slightly with decreasing temperature and reached 65% of the room-temperature value at 10 K. Both line widths and spin susceptibilities are presented in Figure 5.

The temperature behavior of the ESR line width can be qualitatively described with the following model. The Elliott

(21) Kataev, V.; Winkel, G.; Khomskii, D.; Wohlleben, D.; Crump, W.; Tebbe, K. F.; Hahn, J. *Solid State Commun.* **1992**, *83*, 435.
(22) Urayama, H.; Yamochi, H.; Saito, G.; Sugano, T.; Kinoshita, M.; Inabe, T.; Mori, T.; Maruyama, Y.; Inokuchi, H. *Chem. Lett.* **1988**, 1057.
(23) Wang, H. H.; Carlson, K. D.; Geiser, U.; Kini, A. M.; Schultz, A. J.; Williams, J. M.; Welp, U.; Darula, K. E.; Hitsman, V. M.; Lathrop, M. W.; Megna, L. A.; Mobley, P. R.; Yaconi, G. A.; Schirber, J. E.; Overmyer, D. L. *Mater. Res. Soc. Symp. Proc.* **1992**, *247*, 471.
(24) Sugano, T.; Saito, G.; Kinoshita, M. *Phys. Rev. B: Condens. Matter* **1986**, *34*, 117.
(25) Montgomery, L. K.; Geiser, U.; Wang, H. H.; Beno, M. A.; Schultz, A. J.; Kini, A. M.; Carlson, K. D.; Williams, J. M.; Whitworth, J. R.; Gates, B. D.; Cariss, C. S.; Pipan, C. M.; Donega, K. M.; Wenz, C.; Kwok, K. W.; Crabtree, G. W. *Synth. Met.* **1988**, *27*, A195.

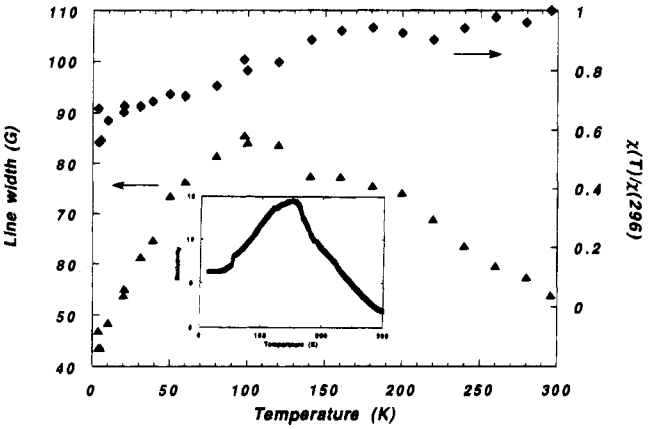

Figure 5. Variable-temperature peak-to-peak line widths (triangles) and relative spin susceptibilities (diamonds) of the κ_L-$(ET)_2Cu(CF_3)_4$-(TCE) phase.

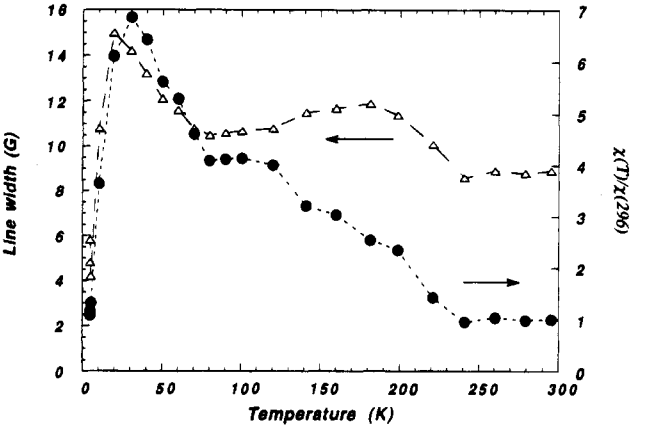

Figure 6. Apparent peak-to-peak line widths (triangles) and relative spin susceptibilities (circles) of the κ_H-$(ET)_2Cu(CF_3)_4$(TCE) needle-phase at low temperatures.

formula gives the correlation between peak-to-peak line width and spin-relaxation time due to spin-orbit coupling in the tight-binding case:[26,27]

$$\Delta H \propto \frac{(\Delta g)^2}{\tau} = \frac{(\Delta g)^2 ne^2}{\sigma m} = \left[\frac{ne^2(\Delta g)^2}{m}\right]\rho \qquad (3)$$

where ΔH is the line width, $\Delta g = g - 2.0023$ (the difference between the observed g value and g value of a free electron), and τ is the relaxation time. Even though Elliott's formula was not designed for low-dimensional metals, and it does not describe the angular dependence well, it may still be applicable to the temperature dependence of a stationary sample. Since the relaxation time of a conduction electron in a metal is proportional to the conductivity, σ, and inversely proportional to the resistivity, ρ,[28] and Δg is constant in a stationary sample (i.e., our experimental condition), the line width should be approximately proportional to the resistivity. This is indeed the case when the observed line widths (this work) are compared with previously reported four-probe resistivity results.[12] The apparent maximum in both resistivity and ESR line width (Figure 5) is a common feature of most of the κ-phase superconducting salts, but its origin is not yet fully understood.[2,20]

The relative spin susceptibility was approximately constant between room temperature and 100 K, with a slight decrease below 100 K. This behavior is consistent with Pauli paramagnetism of a metallic sample.[28] Also noteworthy was the observation of a narrower unresolved absorption line superimposed on the major signal below ~100 K. This narrower peak became sharp and was resolved at 10 K. On the basis of its line width (1.2 G) and intensity, it consisted only of 0.03% of the total integrated absorption. The origin of this sharp line is unknown, but similar sharp lines attributed to crystal defects were also reported for κ-$(ET)_2Cu(NCS)_2$[22] and κ-$(ET)_2Cu[N(CN)_2]Br$.[20]

2. κ_H-$(ET)_2Cu(CF_3)_4$(TCE). The low-temperature ESR behavior of a needle-phase crystal, κ_H-$(ET)_2Cu(CF_3)_4$(TCE) (a sample different from that used in the orientation study), was also measured at the 90° orientation. The line width increased slowly from 9 G at 295 K to ~15 G at 20 K. Below 20 K, the line width dropped precipitously (Figure 6).

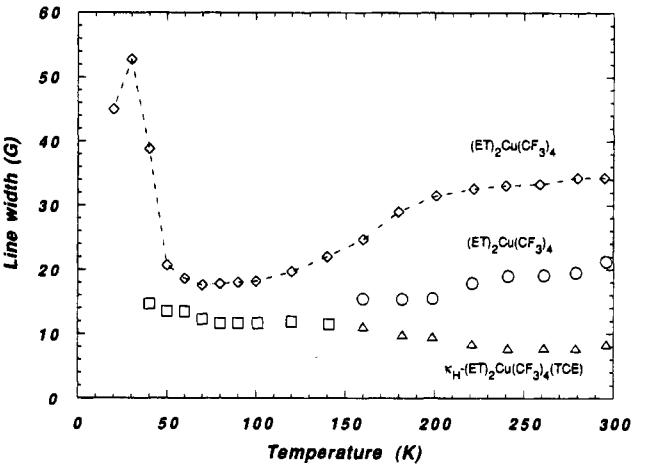

Figure 7. Temperature dependence of the two components of the ESR line width of the κ_H-$(ET)_2Cu(CF_3)_4$(TCE) needles: κ_H-$(ET)_2Cu(CF_3)_4$(TCE) (triangles) and $(ET)_2Cu(CF_3)_4$ (circles). Below 160 K, the spectra cannot be resolved into two components and only the overall line width is shown (squares). Also indicated are the variable-temperature line widths of a pristine sample of $(ET)_2Cu(CF_3)_4$ (diamonds).

The spin susceptibility calculated from the width and intensity of the apparent single signal increased strongly with decreasing temperature below 300 K and reached ~700% of its room-temperature value at 30 K. This behavior is that of a paramagnetic system with localized spins but not of a superconductor. This paradox was resolved when the exact line shape was taken into consideration, and the peak was found to be again a superposition of two transitions observed in the low-temperature data. The results are presented in Figures 7 and 8, for peak-to-peak line width and relative spin susceptibility, respectively. Also plotted are the corresponding values for $(ET)_2Cu(CF_3)_4$ for comparison. The ESR components of the as-grown κ_H phase were interpreted as follows: an 8 G phase attributed to the κ_H-$(ET)_2Cu(CF_3)_4$(TCE) phase and a 20 G phase corresponding to incorporated crystallites of the solvent-free $(ET)_2Cu(CF_3)_4$ phase. The assignment was based on the line widths as well as the much larger spin susceptibility associated with the broader component. These two components were clearly resolved above 160 K, below which temperature the line widths of the two phases became comparable and could not be separated because of high correlations between the fitting parameters. Clearly, the analyzed results indicated that the increasing overall spin susceptibility was dominated by the $(ET)_2Cu(CF_3)_4$ phase and was not an intrinsic effect arising from the superconducting component, κ_H-$(ET)_2Cu(CF_3)_4$(TCE). The

(26) Elliott, R. J. *Phys Rev.* **1954**, *96*, 266.
(27) Sugano, T.; Saito, G.; Kinoshita, M. *Phys. Rev. B: Condens. Matter* **1987**, *35*, 6554.
(28) Kittel, C. *Introduction to Solid State Physics*, 5th ed.; Wiley: New York, 1976.

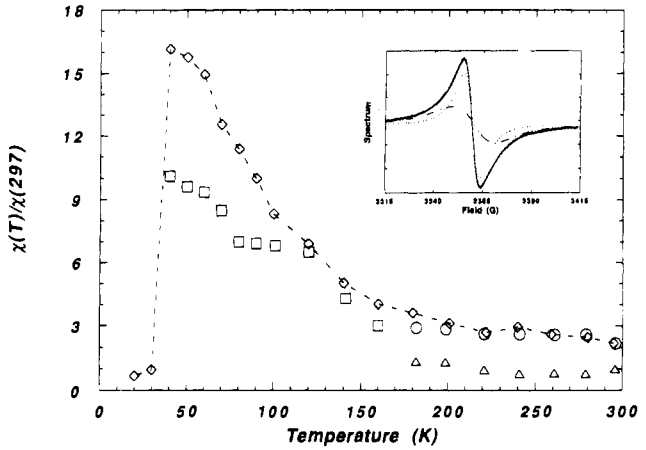

Figure 8. Analyzed spin susceptibility data of the κ_H-$(ET)_2Cu(CF_3)_4(TCE)$ phase showing two components: κ_H-$(ET)_2Cu(CF_3)_4$(TCE) (triangles) and $(ET)_2Cu(CF_3)_4$ (circles). The spin susceptibilities of the unresolved spectra and a separate pristine $(ET)_2Cu(CF_3)_4$ sample are shown with squares and diamonds, respectively. Inset: An actual spectrum at 200 K indicating the 8 G and 20 G components.

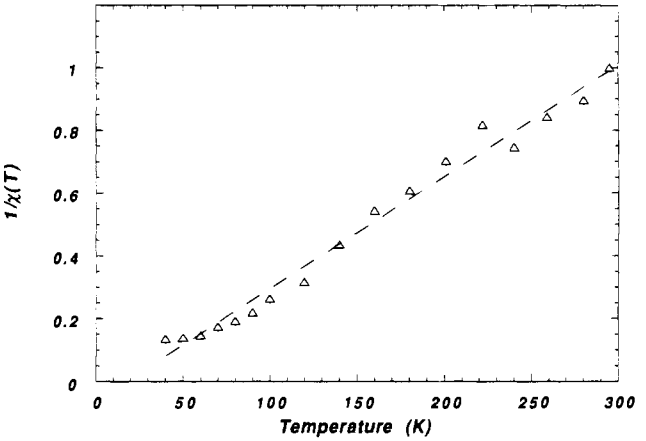

Figure 9. Plot of the inverse spin susceptibility of $(ET)_2Cu(CF_3)_4$ against temperatures showing Curie–Weiss behavior.

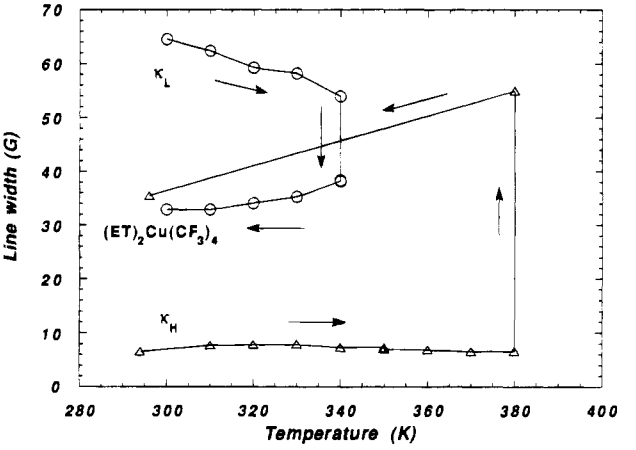

Figure 10. High-temperature-phase transitions of the κ_L- and κ_H-$(ET)_2Cu(CF_3)_4$(TCE) samples indicating conversion temperatures at 340 and 380 K, respectively.

line shape analysis was not carried out below 40 K due to signal distortion caused by the presence of an additional superimposed sharp peak similar to that observed in the κ_L-$(ET)_2Cu(CF_3)_4$(TCE) compound and because of the phase transition of $(ET)_2Cu(CF_3)_4$ (*vide infra*). A low-field scan was also carried out between 20 and 70 G. A weak low field microwave absorption (LFMA) signal[23,29,30] was observed below 8.5 K and disappeared above 9.8 K. The presence of the LFMA signal was consistent with the reported onset of superconductivity in the needle (κ_H) phase near 9 K.[12]

3. $(ET)_2Cu(CF_3)_4$. The low-temperature ESR spectra of $(ET)_2Cu(CF_3)_4$ were measured between 300 and 4 K at the 90° orientation. The line width (Figure 7) decreased from 35 G at ambient temperature to a minimum of ~17 G at 70 K. Below 70 K, the sample underwent a transition, and the line width reached a maximum of 53 G at 30 K and then decreased again to 45 G at 20 K. Below 20 K, the line shape was complicated by the appearance of an extra sharp peak which consisted of ~3% of the total integrated area. The spin susceptibility (Figure 8) showed a monotonic increase upon cooling to ~700% of the room-temperature value at 40 K. The spin susceptibility between 300 and 40 K was fitted with the Curie–Weiss equation (Figure 9)

$$\frac{1}{\chi} = \frac{1}{C}(T + \Theta) \qquad (4)$$

where $C = Ng^2\beta^2/4k$ and Θ is the nonzero Weiss term.[19] Below 40 K, χ dropped by more than one order of magnitude, indicative of a phase transition to a nonmagnetic ground state.

(C) High-Temperature Study. In order to investigate the relationship among the three ET/$Cu(CF_3)_4^-$ phases, high-temperature ESR measurements were carried out in a search for possible thermal phase transitions. Previously, crystals of the semimetallic α-$(ET)_2X$ phase ($X^- = I_3^-$, IBr_2^-) were thermally converted to the corresponding superconductors, β-$(ET)_2X$.[31–33] A crystal of κ_L-$(ET)_2Cu(CF_3)_4$(TCE) was oriented in the ESR cavity at a random orientation and wedged into place with a piece of cotton in order to prevent sample movement. The temperature was slowly raised from 300 K in 10 K increments. As shown in Figure 10, the peak-to-peak line width gradually decreased from 65 G at 300 K to 54 G at 340 K while the spin susceptibility (not shown) remained approximately constant. At 340 K, an abrupt decrease in the line width to 38 G and a sharp increase in the spin susceptibility were observed. After the sample was maintained at 340 K for ~15 min, the temperature was reduced to room temperature in 10 K decrements. The line width decreased to ~33 G at 300 K, while the relative spin susceptibility became 3 times its original value before the thermal cycling, indicating that a thermal phase transition had occurred.

The high-T_c needle phase was also subjected to a similar thermal cycling and was monitored with the use of an ESR spectrometer. Four to five needles of the κ_H-$(ET)_2Cu(CF_3)_4$-(TCE) sample were oriented vertically and grouped together with a piece of cotton in a capillary tube. The sample was heated above room temperature in 10 K increments. The line width showed a very small variation between 300 and 380 K, and the spin susceptibility decreased slightly with increasing temperature. At 380 K, the ESR signal began to broaden,

(29) Romanyukha, A. A.; Shvachko, Y. N.; Skripov, A. V.; Ustinov, V. V. *Phys. Status Solidi B* **1989**, *151*, K59.
(30) Adrian, F. J.; Cowan, D. O. *Chem. Eng. News* **1992**, *70* (Dec 21), 24.
(31) Baram, G. O.; Buravov, L. I.; Degtyarev, L. S.; Kozlov, M. É.; Laukhin, V. N.; Laukhina, E. É.; Onishchenko, V. G.; Pokhodnya, K. I.; Sheinkman, M. K.; Shibaeva, R. P.; Yagubskii, É. B. *Pis'ma Zh. Eksp. Teor. Fiz.* **1986**, *44*, 293 (Engl. Transl. *JETP Lett.* **1986**, *44*, 376).
(32) Schweitzer, D.; Bele, P.; Brunner, H.; Gogu, E.; Haeberlen, U.; Hennig, I.; Klutz, I.; Swietlik, R.; Keller, H. J. *Z. Phys. B: Condens. Matter* **1987**, *67*, 489.
(33) Wang, H. H.; Carlson, K. D.; Montgomery, L. K.; Schlueter, J. A.; Cariss, C. S.; Kwok, W. K.; Geiser, U.; Crabtree, G. W.; Williams, J. M. *Solid State Commun.* **1988**, *66*, 1113.

reaching a line width of 55 G after approximately 15 min. The sample was cooled to room temperature, and the resulting spectrum had a 36 G peak-to-peak line width.

In summary, the behavior of both the κ_L- and κ_H-phases may be explained by the loss of cocrystallized TCE solvent with concomitant conversion to the semiconducting phase, $(ET)_2Cu(CF_3)_4$.

Conclusion

The ESR properties, including angular- and temperature-dependent g values, peak-to-peak line widths, and relative spin susceptibilities of the κ_L-$(ET)_2Cu(CF_3)_4$(TCE) phase (T_c = 4.0 K), are consistent with those of other reported κ-phase salts, such as κ-$(ET)_2Cu[N(CN)_2]X$ (X = Cl, Br)[20,21] and κ-$(ET)_2Cu_2(CN)_3$.[23] The κ_H-$(ET)_2Cu(CF_3)_4$(TCE) sample (T_c = 9.2 K) is a mixture of the pure phase with semiconducting $(ET)_2Cu(CF_3)_4$, and the mixture percentages are sample dependent. The apparent room-temperature angular-dependent g values and line widths of the as-grown κ_H-$(ET)_2Cu(CF_3)_4$(TCE) needles are represented by the major component κ_H-$(ET)_2Cu(CF_3)_4$(TCE) phase. The low-temperature ESR properties of the κ_H-$(ET)_2Cu(CF_3)_4$(TCE) phase are obscured by the strongly paramagnetic $(ET)_2Cu(CF_3)_4$ phase and can only be extracted by use of a careful line shape analysis.

Both κ_L- and κ_H-phases lose cocrystallized solvent at temperatures above ambient and are converted to the semiconducting $(ET)_2Cu(CF_3)_4$ phase. We have previously observed the slow disappearance of superconductivity in the solvated phases because of solvent loss upon standing for longer periods of time at room temperature.[14] Whether the trihaloethane solvent molecules can be reintercalated into the non-solvent-containing $(ET)_2Cu(CF_3)_4$ phase under high pressure, or with the use of large excess amount of solvent, will be the subject for future studies.

Acknowledgment. Work at Argonne National Laboratory was sponsored by the U.S. Department of Energy, Office of Basic Energy Sciences, Division of Materials Sciences, under Contract W-31-109-ENG-38, and research at the University of Cologne was supported by the Fonds der Chemischen Industrie and the Deutsche Forschungsgemeinschaft.

Appendix

(A) The equations used for line shape analysis are listed as follows:[18] (1) a one-line Lorentzian derivative fit

$$Y'(H) = \frac{16IA}{[3 + A^2]^2} + C$$

$$A = \frac{H - H_0}{\frac{1}{2}\Delta H_{pp}}$$

where the four variables are I intensity of the ESR absorption, H_0 center of the absorption, ΔH_{pp} peak-to-peak line width, and C a constant to compensate for the vertical displacement; (2) a two-line Lorentzian derivative fit

$$Y'(H) = \frac{16I_1A_1}{[3 + A_1^2]^2} + \frac{16I_2A_2}{[3 + A_2^2]^2} + C$$

$$A_1 = \frac{H - H_{01}}{\frac{1}{2}\Delta H_{pp1}} \qquad A_2 = \frac{H - H_{02}}{\frac{1}{2}\Delta H_{pp2}}$$

where the seven variables are I_1 and I_2 intensities of the ESR absorption peaks 1 and 2, H_{01} and H_{02} centers of the absorption peaks 1 and 2, ΔH_{pp1} and ΔH_{pp2} peak-to-peak line widths of the absorption peaks 1 and 2, and C a constant to compensate for the vertical displacement.

(B) Equation 1 is entirely equivalent to the following equation which is intuitively easier to understand:

$$g_{obs}^2 = g_{||}^2 \sin^2(\theta + \phi) + g_{\perp}^2 \cos^2(\theta + \phi) \qquad (5)$$

where ϕ is a small angle offset (<1°) to allow for a slight orientation mismatch. When ϕ is near zero, eq 5 is reduced to

$$g_{obs}^2 = g_{||}^2 \sin^2\theta + [{}^1/_2(g_{||}^2 - g_{\perp}^2) \sin 2\phi] \sin 2\theta + g_{\perp}^2 \cos^2\theta$$

The term "$[{}^1/_2(g_{||}^2 - g_{\perp}^2) \sin 2\phi]$" is equivalent to "$g_x^2$" in eq 1.

IC9506421